



## STATE OF CHARGE AS A GOVERNING FACTOR IN VOLTAGE HYSTERESIS FOR SILICON-BASED LI-ION BATTERIES

*Ayesha Fatima Thompson*

Department of Mechanical Engineering, School of Engineering and Computer Science (ENCS),  
Washington State University, Vancouver, WA, United States.

**Abstract:** *This work investigates voltage hysteresis in lithium half-cells using three types of silicon anodes: porous, nano, and bulk. Initial and final capacity differences observed during lithiation–delithiation cycling are corrected using a side-reaction compensation method based on Tafel kinetics. Despite this correction, a notable voltage hysteresis remains across all cell types. To uncover the origin of this hysteresis, we develop a physics-based model incorporating hydrostatic stress. Simulations reveal that stress-induced voltage contributions are minimal and insufficient to account for the observed hysteresis. We further explore how exchange current density varies with the state of charge (SOC) by proposing three SOC-dependent models: average, linear, and logarithmic. Among these, the logarithmic model most accurately replicates the experimental voltage curves, effectively minimizing hysteresis. These findings highlight the limited role of mechanical stress and the dominant influence of electrochemical kinetics on voltage behavior. This study advances the understanding of voltage hysteresis in silicon anode lithium cells and suggests modeling approaches to reduce its impact.*

**Keywords:** *Silicon Anodes, Voltage Hysteresis, Exchange Current Density, State of Charge*

### INTRODUCTION

Lithium-Ion Batteries (LIBs) are regarded as most renowned energy storage capacity systems for electronic devices and heavy electric vehicles (Zhang, 2011). It has been suggested that the performance of the Lithium-Ion batteries can be improved significantly if the graphite in anode can be replaced with silicon (Si) as silicon has much high energy density and high specific capacity (Ashuri et al., 2016; Li et al., 2014) than traditional graphite. However, there are some problems associated with silicon (Si). Si experiences a huge volume expansion (~300%) during lithiation and contraction during delithiation cycling (Di Leo et al., 2015). The stresses generated with these large volume changes have been recognized as the reason for surface cracking and pulverization of silicon electrodes that leads to loss of electrical conductivity and capacity fading during battery cycling (Baker et al., 2017). During lithiation-

delithiation battery cycling experiment in silicon anode-based LIBs, a voltage gap known as voltage hysteresis is witnessed. This hysteresis is detrimental for the health of the batteries.

To optimize the silicon anode battery design, a simple physics-based mathematical model that can predict this reason behind these problems in silicon is required. In the past, various researchers have developed single spherical particle mathematical model on silicon anode-based LIBs (Yang et al., 2014;

Hossain et al., 2020b; Cheng and Verbrugge, 2008; Jin et al., 2019). However, nobody used any experimental data to validate their model. It was also stated that Silicon (Si) particle experiences volume expansion during lithiation. None of the model developers have taken this phenomenon into their account. Battery scientists earlier reported that key parameters cannot remain constant during battery cycling (Li et al., 2014). Nobody has considered this case under their research while developing mathematical model. In our work, we included all these key features in model development. Here, a physics-based electrochemical model has been developed which can mathematically predict the cause behind this voltage hysteresis generation. A modified version of Butler-Volmer (BV) equation including voltage stress induced voltage term as well as Jin et al. (2019) has been developed. Cheng and Verbrugge (2008) developed an analytical solution to calculate hydrostatic stress. We used their analytical solution to calculate stress induced voltage. Here, our principal target is to figure out the main reason behind this voltage hysteresis during lithiation-delithiation battery cycling in silicon anode-based lithium-ion batteries by developing our own mathematical model.

Firstly, three different types of silicon cells (Porous, Nano and Bulk) were prepared by our collaborators. Thereafter, lithiation-delithiation battery cycling experiments were conducted on these three types of coin cell. During battery cycling, some by-products were generated on the interphase of the electrolyte and anode as capacity differences has been witnessed. In order to get rid of this capacity differences, Side-Reaction (SR) rectification was required. Side-reaction correction was done by implementing Tafel regime. Next, one dimensional, half-cell, single particle physics based electrochemical model was developed to validate the experimental results. In the past, Jin et al. (2019) in their work, proposed hydrostatic stress generated from volumetric changes was the main reason of this voltage gap. However, it was necessary to recheck by conducting our own experiment and building mathematical model, whether hydrostatic stress is the main reason, or any other parameters are associated with this voltage hysteresis generation. Therefore, parametric sensitivity analysis was conducted and key parameters figured out. By controlling these parameters as a function, generated voltage hysteresis was successfully minimized during lithiation-delithiation battery cycling. New sets of exchange current density equations were developed. We are the first one in this field to develop new sets of theories related with exchange current density. We created three new sets of equation (linear, logarithmic, and average) and implemented these equations as function of state of charge (SOC) in our model development. It was noticed that logarithmic equation of exchange current density as a function of SOC fits best with our experimental result. From this observation, there was a clear indication that, exchange current density is the most important parameter which is the main reason for voltage hysteresis generated during battery cycling. The impacts of stress induced voltage on voltage hysteresis were also checked. As the present study progresses more elaborate explanation will emerge.

## EXPERIMENTAL

### Battery cycling test

Three different types of cells were manufactured for us by our collaborators. Thereafter, battery cycling was done for all three different types of cells. First, we lithiated the battery to lowest cut off 0.099 [V] then again delithiated back to highest cut off 1.2 [V] without any rest. After lithiation-delithiation

process, one entire cycle was completed. Further, specific capacity was calculated for each voltage point of all the cycles for all three different types of cells and then the capacities were normalized by dividing each point with maximum capacity. In this experiment, measured 0.054 [mA] current was applied.

### Side reaction correction

During battery cycling, each time capacity differences between starting and ending point of the cycle were noticed as shown in Figure 1a. These capacity differences were generated because of the side-reactions as by-products were formed when Tafel chemical kinetics occurred at the interphase between electrolyte and anode. We can reduce this capacity differences by implementing sidereaction correction formula on the exchange current densities (Sethuraman et al. 2012; Hossain, 2020). Sethuraman et al. (2012) applied Tafel regime formula for SR correction in their research. Same formulas were applied in the experiment for the side reaction correction on the exchange current density.

$$i_{0,SR} = i_0 * \exp\left(\frac{\alpha_{SR} F}{RT} (V - U_{SR})\right) \quad (1)$$

The transfer coefficient for the side reaction,  $\alpha_{SR}$ , was assumed to be 0.5 (Hossain et al., 2020a). While, Tafel kinetics did not provide an clear balance potential ( $i_0$  and  $U$  are related), A value of  $U_{SR} = 0.8$  vs. Li/Li<sup>+</sup> was assumed to estimate  $i_{0,SR}$  (Sethuraman et al. 2012; Li et al., 2012; Hossain, 2020). Then, we calculated the side- dots denote delithiation.

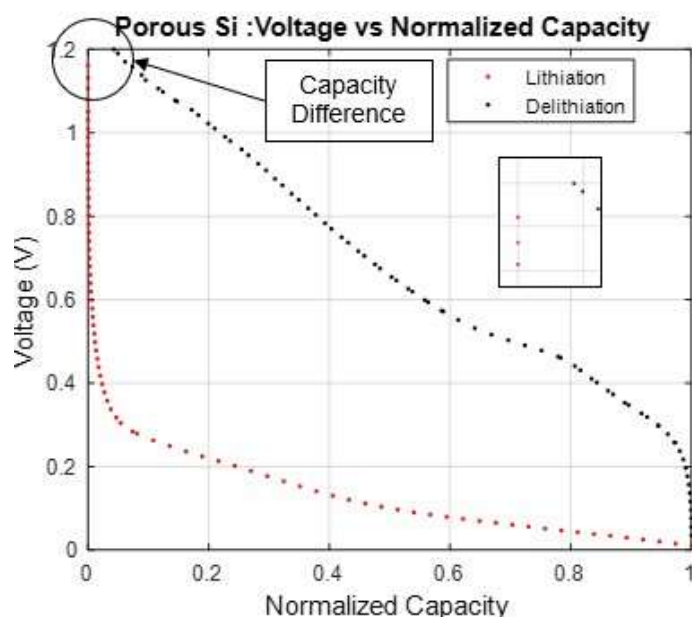


**Figure 1a.** Voltage vs Normalized Capacity before Side Reaction Correction. Red dots indicate Lithiation and Black dots denote delithiation.

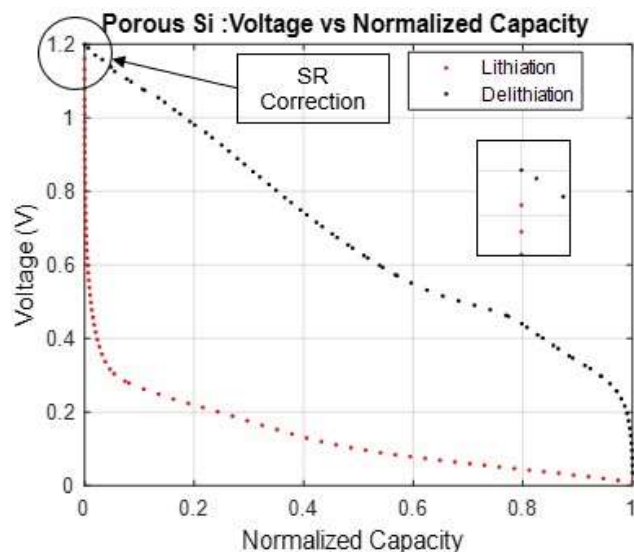


**Figure 1b.** Voltage vs Normalized Capacity after Side Reaction Correction. Red dots indicate Lithiation and Black voltage hysteresis.

### Voltage hysteresis

We produced Voltage [V] vs Normalized Capacity graphs for silicon anode-based LIBs as it is presented in the Figure 2a and 2b.

From Figure 2a, it is clear that, huge voltage hysteresis was created on silicon anode cell during battery cycling. Whereas, in case of graphite anode, voltage gap generation was almost insignificant (Figure 2b).

From, this experiment, it was evident that, voltage hysteresis generation is a specific occurrence in silicon anode-based lithiumion batteries.

In this current work, we want to mathematically investigate the reason behind this voltage hysteresis generation. So, our objective in this work was to mathematically scrutinize the reason behind this voltage hysteresis phenomenon. Therefore, we developed a physics based one dimensional single spherical particle mathematical model and investigated the cause of voltage hysteresis occurrence.

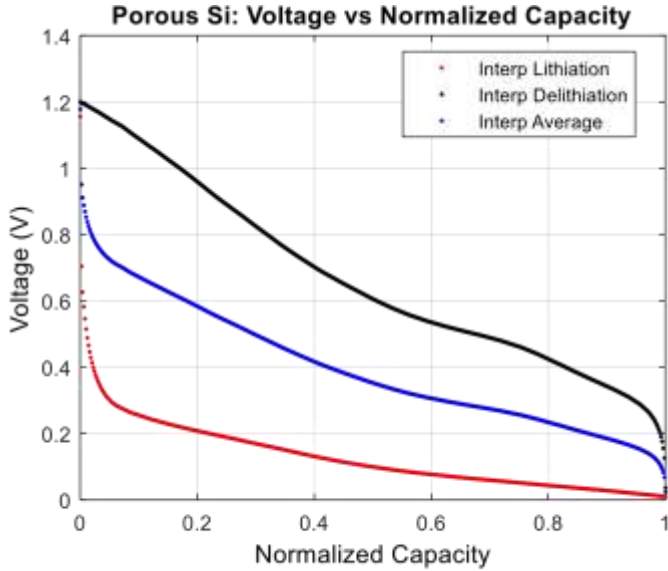


**Figure 2a.** Battery cycling experiment of silicon anode-based lithium-ion half cells. Huge voltage gap is noticed. It is called **Graphite Cell: Voltage vs Normalized Capacity**

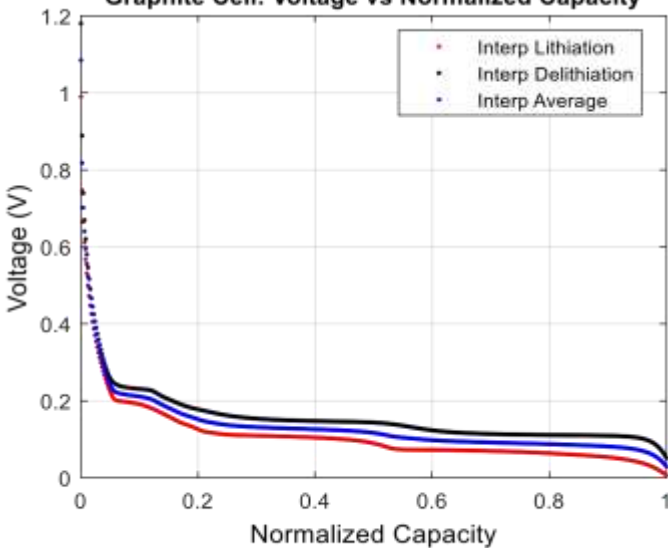


**Figure 2b.** Battery cycling experiment of graphite anode-based

## Model development

### Mass balance equation

Since our current mathematical model is a single particle one- dimensional half-cell model, the model developed in this study assumed the silicon particle to be a single-phase system. The governing equations and boundary conditions (Table 1) for this model have been discussed in the paper. These equations are comprised of mass balance in the solid phases and the modified Butler-Volmer equation coupled with hydrostatic stress induced voltage to describe the core electrochemical reaction at the interfaces. The hydrostatic stress in the surface layer due to surface effects was comprised of two different sections. One depended on the average concentration  $c_{av}(R)$  which means that the diffusion

induced deformation. The other one was concentration independent. To estimate diffusion coefficients in the particle using data, we numerically solved Fick's law (Equation 2) in spherical coordinates.

**Table 1.** Governing equations and boundary conditions for porous electrode (half-cell) model.

Governing equations	Boundary conditions
Mass balance in solid phase (spherical coordinate) ( $c_s$ : lithium concentration)	
$\frac{\partial c_s}{\partial t} = D \frac{\partial^2 c_s}{\partial r^2} + 2 \frac{D}{r} \frac{\partial c_s}{\partial r}$	$D \frac{\partial c}{\partial r} \big _{r=R} = -\frac{i_{app}(t)}{a_V L F} ; D \frac{\partial c}{\partial r} \big _{r=0} = 0$
Average concentration profile in solid phase	
$\epsilon F L \frac{dc_{av}(t)}{dt} = i_{app}(t)$	
Modified Butler-Volmer voltage equation	
$V = U + \frac{\sigma_h \Omega}{F} + \frac{2RT}{F} \sinh^{-1} \left( \frac{i_{app}(t)}{2i_0 a_V L F} \right)$	

$$\frac{\partial c_s}{\partial t} = D_s \frac{\partial^2 c_s}{\partial r^2} + 2 \frac{D_s}{r} \frac{\partial c_s}{\partial r} \quad (2)$$

The boundary and initial conditions are (Figure 3),

$$D \frac{\partial c_s}{\partial r} = -\frac{i_{app}(t)}{a_V L F} \quad \text{for } r = r_0 \quad (3)$$

$$D \frac{\partial c_s}{\partial r} = 0 \quad \text{for } r = 0 \quad (4)$$

$$c_{s,0} = c_0 \quad \text{for } t = 0 \quad (5)$$

Where  $r_0$  is the particle radius [m],  $c_s$  is the lithium concentration [mol/m<sup>3</sup>],  $c_{s,0}$  is the initial lithium concentration [mol/m<sup>3</sup>],  $D_s$  is the diffusion coefficient [m<sup>2</sup>/s],  $i_{app}$  is the current density [A/m<sup>2</sup>],  $a_V$  is the surface-to-volume ratio [1/m],  $L$  is cell thickness [m],  $F$  is the Faraday's constant [C/mol].  $i_{app}(t)$  is denoted as applied current as a function of time. In estimating the diffusion coefficients, both particle volume changes and stress effects were ignored.

### Modified Butler-Volmer equation

In this model, hydrostatic stress induced voltage in Butler-Volmer (BV) equation was included. The electrode particle goes all the way through the volumetric strain during the lithiation/delithiation battery cycling that results in stress generation inside the spherical particle. This stress generation due to lithium battery cycling in the electrode particle is calculated by the hydrostatic stress as reported by Cheng and Verbrugge (2008). The Butler-Volmer equation can be expressed,

$$j_n = \frac{i_0}{F} \left\{ \exp \left[ \frac{F(V-U)-\sigma_h \Omega}{2RT} \right] - \exp \left[ -\frac{F(V-U)-\sigma_h \Omega}{2RT} \right] \right\} \quad (6) \quad j_n \text{ is net flux [mol/m}^2\text{/s]}. \text{ It is defined as}$$

$$j_n = \frac{i_{app}(t)}{a_V L F} \quad (7)$$

Therefore, Equation (6) can be expressed as follows,

$$\frac{i_{app}(t)}{a_V L F} = \frac{i_0}{F} \left\{ \exp \left[ (1-\alpha) \frac{F(V-U)-\sigma_h \Omega}{RT} \right] - \exp \left[ -\alpha \frac{F(V-U)-\sigma_h \Omega}{RT} \right] \right\} \quad (8)$$

Where,  $\sigma_h$  is hydrostatic stress at the surface layer of electrode, [N/m<sup>2</sup>],  $\Omega$  is the partial molar volume [m<sup>3</sup>/mol],  $\alpha$  is the symmetric coefficient,  $i_0$  is the exchange current density [A/m<sup>2</sup>],  $R$  is the universal gas constant [J/kg/K],  $T$  is the temperature [K]. If we use  $\alpha = 0.5$ , Equation (8) can be written as,

$$V = U + \frac{\sigma_h \Omega}{F} + \frac{2RT}{F} \sinh^{-1} \left( \frac{i_{app}(t)}{2i_0 a_V L F} \right) \quad (9)$$



Cheng and Verbrugge (2008) developed analytical solution for hydrostatic stress calculation at their work. Expressed as

$$\sigma_h(r_0) = \frac{2E\Omega}{9(1-\nu)} [S_1 c_{av}(r_0) - c_s(r_0)] + S_2 \quad (10)$$

Here,  $S_1$  and  $S_2$  are the constants. These two can be written as:

$$S_1 = \frac{1 - \frac{K^s(1+\nu)}{R} \frac{E}{E}}{1 + \frac{2K^s(1-\nu)}{R} \frac{E}{E}}$$

$$S_2 = -\frac{\frac{2\tau^0}{R}}{1 + \frac{2K^s(1-\nu)}{R} \frac{E}{E}} \quad (11)$$

Where,  $K^s$  is the surface modulus [N/m],  $\tau^0$  is the deformation independent surface tension [J/m<sup>2</sup>],  $E$  is the Young's modulus [GPa],  $\nu$  is Poisson's ratio.  $\sigma_h$  is hydrostatic stress [GPa],  $c_{av}$  is denoted as average lithium concentration [mol/m<sup>3</sup>].  $\sigma_h$  &  $c_{av}$  are used here as variable.

In our physics based mathematical model, we identified key parameters essential for our experimental validation. However, in our work, we developed new sets of equations for exchange current density and make those as a function of state of charge (SOC). Therefore, we implemented these new equations in our model and checked with experimental results. How we developed these key parameters is discussed in the next segment. State of charge (SOC) as defined,

$$SOC = \frac{c_v}{c_{max}} \quad (13)$$

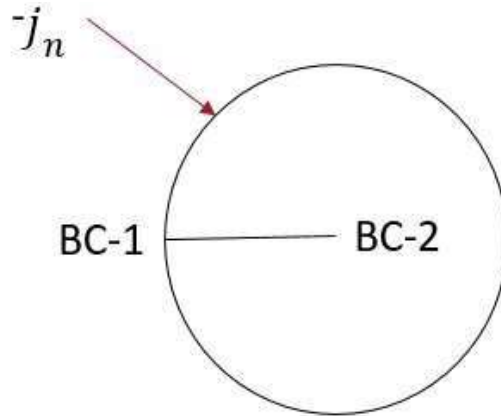


**Figure 3.** Schematic diagram of a spherical particle. Source: Hossain and Kim (2020).

Here  $c_s$  is the lithium concentration [mol/m<sup>3</sup>] and  $c_{max}$  is denoted as maximum concentration [mol/m<sup>3</sup>].

Pharr et al. (2013) studied about surface cracking at the electrode. Surface cracking is directly related with surface-to-volume ratio,  $aV$ . Constant particle radius was used to calculate  $aV$ .

Surface-to-volume ratio could be calculated as below,

$$aV = \frac{N \cdot 4\pi r_0^2}{\frac{1}{\epsilon} N \cdot \frac{4}{3}\pi r_0^3} = \frac{3\epsilon}{r_0} \quad (14)$$

Where,  $\epsilon$  is volume ratio of silicon,  $N$  is the number of particles, here  $N=1$ . Surface-to-volume ratio is an important parameter related with exchange current density.

### **Modified exchange current density**

In our model, instead of going with traditional exchange current density equation, we developed new sets of exchange current density equations. First, we took constant values and made an average as follows,

$$i_{0_{S,SR_{avg}}} = \frac{i_{01} + i_{02}}{2} \quad (15)$$

Next, we developed linear equation for exchange current density as a function of state of charge (SOC) as defined,

$$i_{0_{SOC,SR_{linear}}} = (i_{02} - i_{01})SOC + i_{01} \quad (16)$$

Then, we developed logarithmic equation for  $i_{0,SR}$  as a function of SOC,

$$i_{0_{SOC,SR_{logarithmic}}} = 10^{[\log_{10}(i_{01}) + SOC \log_{10}(i_{02}/i_{01})]} \quad (17)$$

The derivation of Equation 17 is shown in Appendix 1.

In Figure 4, how exchange current density changes with state of charge is shown.

When,  $SOC = 0$ , it defines unlithiated state. In unlithiated state,  $i_{0,SR}$  value is denoted as  $i_{01}$  [A/m<sup>2</sup>]. As, SOC values keep increasing,  $i_{0,SR}$  value goes increasing. Therefore, when we have,  $SOC = 1$ , it indicates fully lithiated state. In this state,  $i_{0,SR}$  value becomes as  $i_{02}$  [A/m<sup>2</sup>].

We used all the equations to check which one matches the best with the experimental result. Equation (15) shows  $i_{0,SR}$  remains constant throughout whereas Equation (16) showed linear increment of exchange current density as a function of SOC and Equation (17) exhibited the logarithmic increment of the same as a function of SOC.

### **Solution procedure**

We implemented all the mathematical model equations and boundary conditions using finite element package COMSOL Multiphysics 5.5. Model parameters such as electrode design, thermodynamics, transport, kinetic, and mechanical properties are listed in Table 1. In our experiment, we completed several complete batteries cycling test in Standard Condition such as 25C (room temperature). For experimental validation, we chose cycle no.9 for all three different types of silicon (porous, nano and bulk) anodebased cell as we found stability in SEI layer formation. The validity of the parameter choice is checked by comparing the physics model to experiments, as shown in Table 2.

### **RESULTS AND DISCUSSION**

In analyzing electrodes at high C-rates, relatively thin layer electrodes are considered as an ideal design as the transport limitations in the electrolyte phase is overlooked. The case is confirmed in our ideal electrode using the porous electrode model. At first, we generated Voltage vs Normalized Capacity graph from our experimental data. Then, we corrected side-reaction generated from chemical kinetics using Tafel regime. Using all the equations we developed in our mathematical model, we tried to validate our experimental result.

From our literature survey and sensitivity analysis, key parameters were identified. All the parameter values were chosen as constant for these key parameters except exchange current density values. We developed three new sets of exchange current density equation as a function of state of charge (SOC) (Equations 15, 16 and 17) and implemented those in our mathematical model and then we tried to match with our experimental result as shown in Figure 5. Here, in Figure 5(a, b and c), red dotted lines



denote experimental result for all three cells [(a) Porous, (b) Nano and (c) Bulk]. Blue solid lines indicate voltage vs normalized capacity generated using logarithmic exchange current density as a function of state of charge (SOC); cyan dashed line defines linear exchange current density as a function of SOC and purple dashed line used to indicate average exchange current density (constant). It can be noticed that Voltage [V] vs Normalized Capacity graph generated with average exchange current density and linear SOC based exchange current density did not match with experimental result. Whereas logarithmic exchange current density equation as function of SOC fitted best with the experimental result of three different kinds of silicon anode (Porous, Nano and Bulk). By changing the values of exchange current density values in Equation 17, the shape of the voltage curve can be changed heavily.

From these observations, it can be clearly seen that by controlling exchange current density, the shape of the voltage curve can be changed. Other key parameters such as solid diffusivity, partial molar volume, Young's modulus, and Poisson's ratio have very low impact on voltage hysteresis.

Next, stress induced voltage ( $\sigma_h \Omega$ ) was calculated and value was found to be approximately  $2 \times 10^{-4}$  [V] for porous cell as the blue line denotes,  $3.5 \times 10^{-4}$  [V] was found for nano cell as the red line denotes and  $4 \times 10^{-4}$  [V] was found for bulk cell as bulk line denotes which quite low to have impact on voltage hysteresis generation as shown in Figure 6. For other cycles of porous, nano, and bulk cell the case was found same. On the other hand, by changing exchange current densities, voltage curves shapes can be controlled. Therefore, it is a clear indication that state of charge (SOC) dependent exchange current density is the key parameter which can control voltage hysteresis generated during lithiation/delithiation battery cycling of silicon anode-based lithiumion batteries. By controlling exchange current density, voltage hysteresis can be minimized.

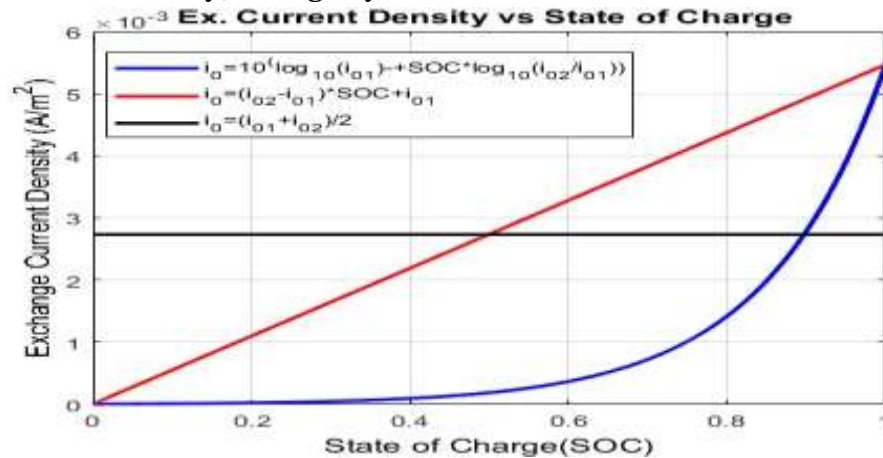


**Figure 4.** Development of three different types of exchange current density equations a function of state of charge (SOC).

**Table 2.** List of model parameters used in this study.

Parameter	Value	Description	References
$r_0$	$500 \times 10^{-9}$	Initial particle radius [m]	Hossain (2020b)
$D_s$	$2 \times 10^{-15}$	Solid diffusivity [m²/s]	"
Capa	Calculated from experiment	Columbic capacity [mAh/g]	Measured

io1		Exchange current density-1 [A/m <sup>2</sup> ]	Hossain (2020b)
io2	$6.46 \times 10^{-6}$ $5.46 \times 10^{-3}$	Exchange current density-2 [A/m <sup>2</sup> ]	“
cmax	$\rho \times \frac{Capa}{F}$	Maximum concentration [mol/m <sup>3</sup> ]	Kim (2014)
C-rate Calculated from experiment C-Rate [1/h] Measured $c_{01} \times \frac{x_{C_{01.4\%}}}{x_{C_{01.4\%}}}$ Initial concentration [mol/m <sup>3</sup> ] “			
E	100	Young's modulus constant [GPa]	Pal (2014)
v	0.27	Poisson's ratio constant	Lu (2016)
ε	0.6517	Volume ratio of silicon	Liang (2014)
L	$116 \times 10^{-6}$	Thickness of electrode [m]	Hossain (2020a)
F	96487	Faraday constant [C/mol]	“
R	8.314	Universal gas constant [J/mol/K]	“
T	298	Temperature [K]	Wu (2012)
ρ	2330	Density of silicon [kg/m <sup>3</sup> ]	“
x <sub>0</sub>	0.0001	Initial SOC of silicon 0.0001	Sikha (2014)
Ω	$4.26 \times 10^{-6}$	Partial molar volume [m <sup>3</sup> /mol]	Song (2016)
K <sup>s</sup>	5	Surface modulus [N/m]	“
τ <sub>0</sub>	1	Deformation-Independent surface tension [J/m <sup>2</sup> ]	“
m	$1.043798 \times 10^{-3}$	Mass of the cell [kg]	Measured

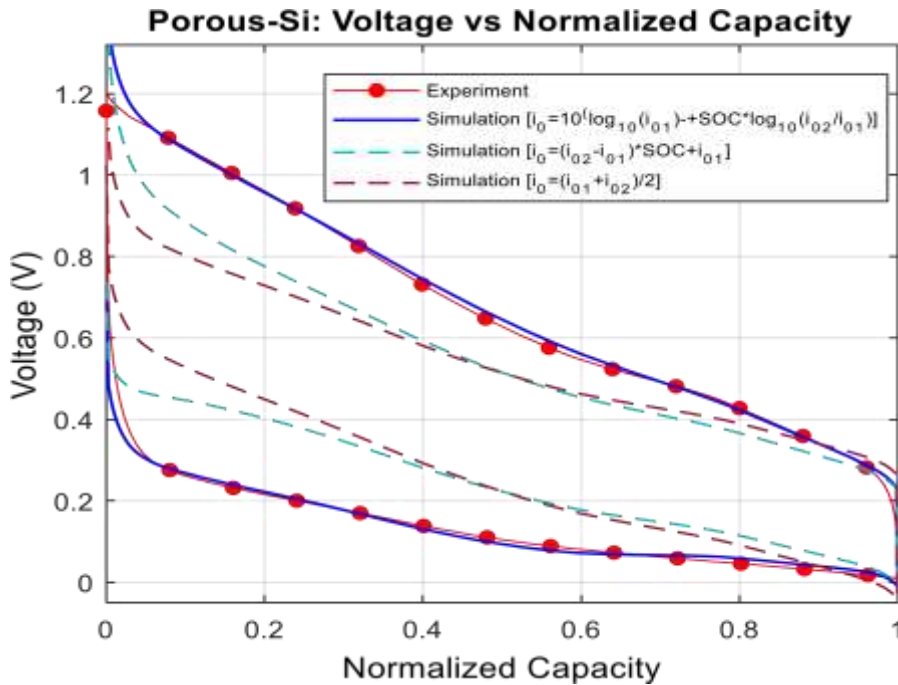


**Figure 5a.** Experimental validation of Voltage vs Normalized Capacity graph for Porous Si Cell.

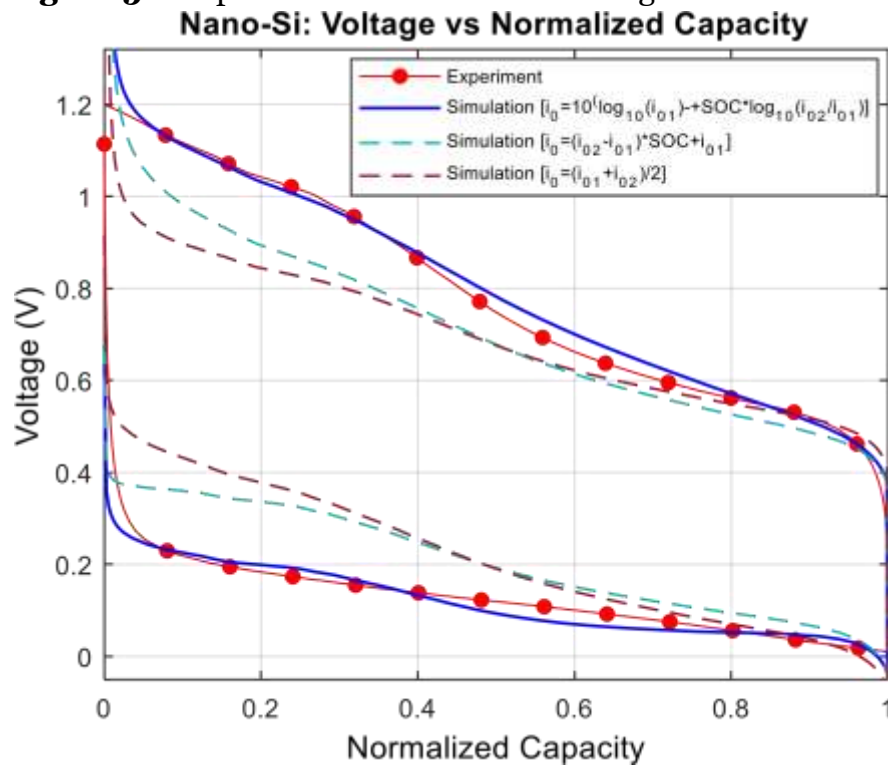


**Figure 5b.** Experimental validation of Voltage vs Normalized Capacity graph for Nano Si Cell.

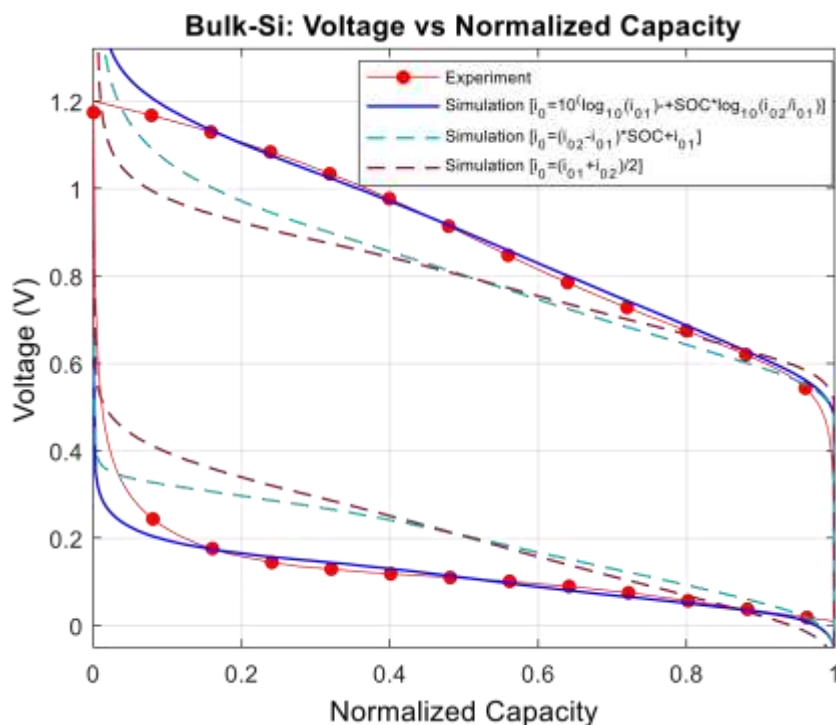


**Figure 5c.** Experimental validation of Voltage vs Normalized Capacity graph for Bulk Si Cell.

### Conclusion

In this work, we thoroughly investigated the cause of voltage gap generation during lithiation-delithiation cycling of silicon anode-based lithium-ion cell at the particle scale by combining experimental and modeling techniques. First, we conducted battery cycling test. Then we corrected the side-reaction on exchange current density using Tafel kinetics. Voltage hysteresis was witnessed during cycling. We developed a physics-based mathematical model to identify the main reason behind this voltage gap. Earlier researchers reported that hydrostatic stress generation is the main cause. In our model, we analyzed hydrostatic stress and noticed that stress induced voltage does not have enough impact with this hysteresis. Next, we identified some key parameters to see the influence on the voltage hysteresis. Doing so, we did not find any influence. Then, we focused on the exchange current and developed new sets of theories based on state of charge (SOC). Significant impacts have been found on the generated voltage hysteresis during battery cycling. With the logarithmic equation of exchange current density as function of SOC, we found the best match with our experimental and simulation results. Simulation results suggested that, state of charged based exchange current density is the most influential parameter for voltage hysteresis generation in silicon anode-based LIBs. So, it can be stated that, exchange current density is the main reason of voltage hysteresis occurrence during lithiation/delithiation battery cycling of silicon anode-based lithium-ion batteries.

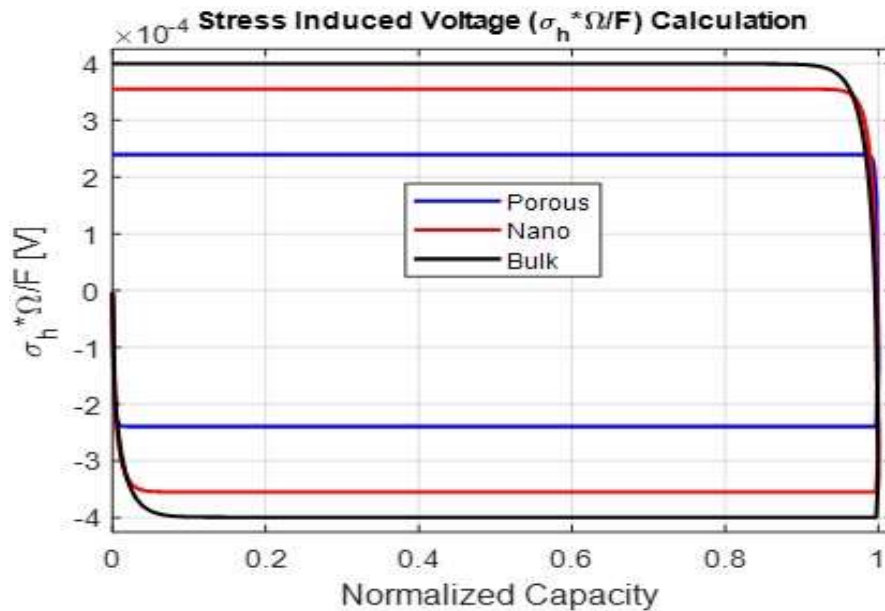


**Figure 6.** Graph plotting of stress induced voltage ( $\sigma_h \Omega/F$ ) vs. normalized capacity.

### CONFLICT OF INTERESTS

The author has not declared any conflict of interests.

### ACKNOWLEDGEMENTS

The authors thank Dr. Sun Ung Kim for permitting the use of Electrochemical Engineering Lab of Washington State University-Vancouver. Dr. Younghwan Cha and Dr. MinKyu Song of Song Research Group of Washington State University-Pullman are also greatly appreciated for providing the three different types of silicon anode-based lithium-ion batteries. All the encouragement and support received are awesome.

### REFERENCES

- Ashuri M, He Q, Shaw L (2016). Silicon as a potential anode material for Li-ion batteries: where size, geometry and structure matter. *Nanoscale* 8(1):74-103.
- Baker D, Verbrugge M, Xiao X (2017). An approach to characterize and clarify hysteresis phenomena of lithium-silicon electrodes, *Journal of Applied Physics* 122(16):165102.
- Cheng YT, Verbrugge MW (2008), The influence of surface mechanics on diffusion induced stresses within spherical nanoparticles, *Journal of Applied Physics* 104(8):083521.
- Di Leo C, Rejovitzky E, Anand L (2015). Diffusion–deformation theory for amorphous silicon anodes: The role of plastic deformation on electrochemical performance, *International Journal of Solids and Structures* 67:283-296.
- Hossain A, Masud N, Yasin M, Ali A (2020a). Analysis of the performance of microbial fuel cell as a potential energy storage device, *International Exchange, and Innovation Conference on*

Copyright: © 2025 Continental Publication

Engineering and Sciences (IEICES) 6 (2020) At: Kyushu University, Fukuoka City, Japan 6:149-155.

Hossain AA (2020). Development of a physics-based mathematical model of microparticle silicon-based lithium half cells, Masters, Washington State University-Vancouver.

Hossain AA, Cha Y, Song M, Kim SU (2020b). Side reaction correction and non-linear exchange current density for mathematical modeling of silicon anode-based lithium-ion batteries.

Hossain AA, Kim SU (2020). Development of a physics-based mathematical model to analyze the limitations of microparticle siliconbased lithium half cells IMECE Technical Presentation.

Jin C, Li H, Song Y, Lu B, Soh A, Zhang J (2019). On stress-induced voltage hysteresis in lithium-ion batteries: Impacts of surface effects and inter-particle compression. Science China Technological Sciences 62:1357-1364.

Kim SU, Albertus P, Cook D, Monroe C, Christensen J (2014). Thermochemical simulations of performance and abuse in 50Ah automotive cells. Journal of Power Sources 268:625-633.

Li J, Dudney N, Xiao X, Cheng Y, Liang C, Verbrugge M (2014). Asymmetric rate behavior of Si anodes for lithium-ion batteries: ultrafast delithiation versus sluggish lithiation at high current densities, Advanced Energy Materials 5(6):1401627.

Li J, Xiao X, Yang F, Verbrugge MW, Cheng YT (2012). Potentiostatic intermittent titration technique for electrodes governed by diffusion and interfacial reaction. The Journal of Physical Chemistry C 116(1):1472-1478.

Liang B, Liu Y, Xu Y (2014). Silicon-based materials as high-capacity anodes for next generation lithium-ion batteries. Journal of Power Sources 267:469-490.

Lu B, Song Y, Zhang Q, Pan J, Cheng Y, Zhang J (2016). Voltage hysteresis of lithium-ion batteries caused by mechanical stress. Physical Chemistry Chemical Physics 18(6):4721-4727.

Pal S, Damle SS, Patel SH, Datta MK, Kumta PN, Maiti S (2014). Modeling the delamination of amorphous-silicon thin film anode for lithium-ion battery. Journal of Power Sources 246:149-159.

Pharr M, Suo Z, Vlassak J (2013). Measurements of the fracture energy of lithiated silicon electrodes of li-ion batteries, Nano Letters 13(11):5570-5577.

Sethuraman V, Srinivasan V, Newman J (2012). Analysis of electrochemical lithiation and delithiation kinetics in silicon, Journal of the Electrochemical Society 160(2):A394-A403.

Copyright: © 2025 Continental Publication

- Sikha G, De S, Gordon J (2014). Mathematical model for silicon electrode - Part I. 2-d model, Journal of Power Sources. 262:514523.
- Song Y, Soh A, Zhang J (2016). On stress-induced voltage hysteresis in lithium ion batteries: impacts of material property, charge rate and particle size. Journal of Materials Science 51(21):9902-9911.
- Wu H, Cui Y (2012). Designing nanostructured Si anodes for high energy lithium-ion batteries. Nano Today 7(5):414-429.
- Yang H, Fan F, Liang W, Guo X, Zhu T, Zhang S (2014). A chemomechanical model of lithiation in silicon, Journal of the Mechanics and Physics of Solids 70:349-361.
- Zhang W (2011). A review of the electrochemical performance of alloy anodes for lithium-ion batteries. Journal of Power Sources 196(1):1324.